PHYSICAL REVIEW B **70**, 121101(R) (2004)

Electron-lattice coupling and broken symmetries of the molecular salt $(TMTTF)_2SbF_6$

W. Yu,[1,*] F. Zhang,[1] F. Zamborszky,[1] B. Alavi,[1] A. Baur,[2]
C. A. Merlic,[2] and S. E. Brown[1]
[1]*Department of Physics and Astronomy, University of California, Los Angeles, California 90095, USA*
[2]*Department of Chemistry and Biochemistry, University of California, Los Angeles, California 90095, USA*
(Received 2 April 2004; revised manuscript received 8 June 2004; published 8 September 2004)

The temperature/pressure phase diagram for $(TMTTF)_2SbF_6$ is determined using ^{13}C NMR spectroscopy. At ambient pressure, a transition to a charge-ordered (CO) state occurs at $T_{CO}=156$ K, and antiferromagnetic (AF) order is observed below $T_N=8$ K. Both are suppressed with pressure: when $P>0.5$ GPa, there is no evidence for CO, and the low-temperature ^{13}C NMR spectrum is consistent with a singlet [spin-Peierls (SP)] ground state. At a given pressure, the temperature dependence of the CO order parameter is not monotonic, and provides an opportunity to identify what processes could be controlling the CO amplitude. ^{19}F NMR spectroscopy provides empirical evidence that electron-counterion coupling is crucial to stabilizing the CO and AF phases.

DOI: 10.1103/PhysRevB.70.121101 PACS number(s): 71.20.Rv, 71.30.+h, 71.45.Lr, 76.60.−k

The isostructural family of charge transfer salts (CTS) $(TMTTF)_2X$ and $(TMTSF)_2X$ are formed with singly charged anions, such as ClO_4^-, PF_6^-, and Br^-, so the average hole count is 0.5 per donor.[1] In the case of the TMTTF salts, they are susceptible to a charge-ordering (CO) transition at temperatures of the order of 100 K,[2,3] that is often attributed to the importance of both on-site and near-neighbor Coulomb repulsion,[4] and influenced by electron-lattice coupling.[3,5–8] Compared to the analog TMTSF materials, the bandwidths are much smaller, and therefore models naturally producing charge order and including only electronic degrees of freedom could be expected to describe some aspects of the physics correctly. Nevertheless, it is unclear whether realistic parameters successfully describe the experiments in several ways. First, it has been argued that the near-neighbor repulsion may not be strong enough to stabilize the charge order.[6,7,9] Furthermore, although the charge-order (CO) order parameter has not been determined directly, there is indirect evidence from transport[10] and electron paramagnetic resonance[11] (EPR) measurements that the order-parameter's wave vector changes when the symmetry of the counterion is changed. An explanation should involve coupling of the charge degrees of freedom on the molecular stacks to the lattice. Calculations on one-dimensional models, including intramolecular, intermolecular, and counterion coupling, indicate that when these degrees of freedom are included, a variety of new broken symmetry states are possible.[6–8] At least in the case of the insulating TMTTF materials, it is not surprising that the robustness of the CO phase influences the ground state symmetry. [12] To date, very little is known about the details of the observed phases and what controls their stability.

The sensitivity to chemical or mechanical pressure of this class of materials provides an opportunity to explore some general trends. Below, we map out the temperature/pressure phase diagram for $(TMTTF)_2SbF_6$ using ^{13}C NMR spectroscopy. The CO/AF ground state found at low pressures is replaced with a singlet state with no detectable CO amplitude beyond $P\approx 0.5$ GPa. This information is used to amend the generic phase diagram for the family of TMTTF/TMTSF CTS, to include the observations from $(TMTTF)_2SbF_6$ at the "low pressure" end. Within the CO state, the CO order parameter does not increase monotonically upon cooling below T_{CO}, but passes through a maximum and then decreases upon further cooling. ^{19}F NMR spectroscopy shows that this behavior coincides with the freezing of counterion motion, and we offer the association of the two observations as evidence for the important role that electron/counterion coupling plays in stabilizing the CO state.

The samples were prepared using the standard electrolysis technique. Spin-labeled TMTTF donors were synthesized with two ^{13}C nuclei on the bridging sites at the center of the dimer molecules,[13] and subsequent crystal growth was carried out by electrolysis. The experiments consist of ^{13}C and ^{19}F NMR spectroscopy on $(TMTTF)_2SbF_6$ as a function of pressure and temperature, with the field applied perpendicular to the ***a*** (molecular stacking) axis. In the first case, the external field was $B_0=9.0$ T, and we used two-dimensional (2D) spin-echo spectroscopy to separate the effects of the strong intramolecular ^{13}C-^{13}C magnetic dipolar coupling from the hyperfine and chemical shifts.[14] For the ^{19}F measurements, $B_0=4.9$ T was used. High pressure experiments were performed using a standard BeCu clamp cell using Fluorinert 75 (3M) for the medium. In all cases, the quoted pressure is derived from the force applied at $T=300$ K, and systematic consistency was verified using separate calibration runs.

Typical ^{13}C 2D NMR spectral changes brought on by the CO phenomenon are illustrated in Fig. 1. The hyperfine and chemical shifts are plotted on the vertical f_2-f_1 axis, and the ^{13}C-dipolar coupling is shown on the horizontal f_1 axis. We note that the frequencies f_1 and f_2 result from the Fourier transform of the two-dimensional data set in (t_1,t_2), as defined in the figure. The spectrum taken with $T<T_{CO}$ is shown directly, and the spectrum for $T>T_{CO}$ is represented by the dark, open circles. Consider first the spectrum of the high-temperature phase. The signal appears at two frequencies, ν_A and ν_B, on the f_2-f_1 axis. When $T<T_{CO}$, the number

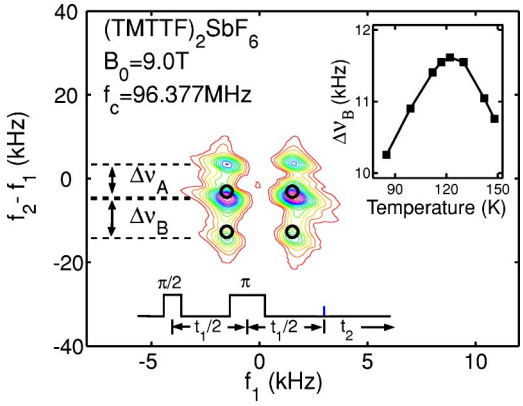

FIG. 1. (Color online) Ambient pressure ^{13}C NMR spectra at temperatures $T=85$ K$<T_{CO}$ (contours) and $T=156$ K$>T_{CO}$ (signal location represented by dark, open circles). The applied field is 9.0 T directed in the $\mathbf{b}'$-$\mathbf{c}^*$ plane. Δf_d is the dipolar coupling frequency between the two inequivalent ^{13}C nuclei in each molecule. In the inset is the temperature dependence of the frequency difference ($\Delta\nu_B$) of the peaks, and is proportional to the CO amplitude.

of signal features double along the f_2-f_1 axis. As an example, the peak at ν_B becomes two that are separated by $\Delta\nu_B$. The separation Δf_d, corresponds to the nuclear dipole coupling strength (for inequivalent nuclei) and remains constant as the temperature is varied.

Contrasting to the ambient pressure results are spectra recorded at pressures beyond $P=0.5$ GPa. An example of a spectrum recorded at $T=2$ K and $P=0.6$ GPa is shown in Fig. 2. There are two striking differences from the low-pressure spectra. First, instead of spots, there appears two very broad features along the f_2-f_1 axis. As before, these are separated along the f_1 axis by the dipolar coupling frequency Δf_d.[15] Second, there appear two spots, at the same frequency on the f_2-f_1 axis, but separated by $(3/2)\Delta f_d$ on the f_1 axis.

We switch briefly to results from ^{19}F NMR spectroscopy, and return to the ^{13}C data in the discussion. These are shown in Fig. 3. The spectra were recorded for a range of temperatures covering T_{CO}, and in an applied field of $B=4.91$ T. Two examples of the spectra appear in the inset. At high temperatures, the line is homogeneously broadened and Gaussian in

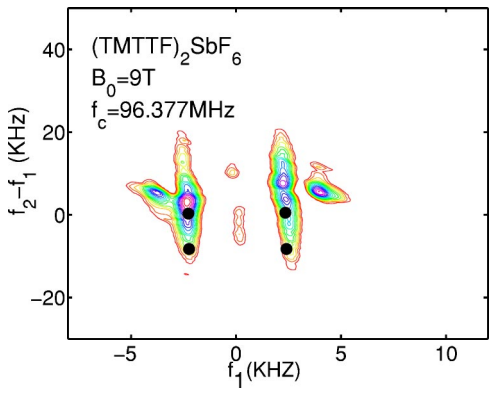

FIG. 2. (Color online) ^{13}C NMR spectra at $T=2$ K (contours) and $T=30$ K (signal location represented by dark, closed circles) with loading pressure $P=0.6$ GPa.

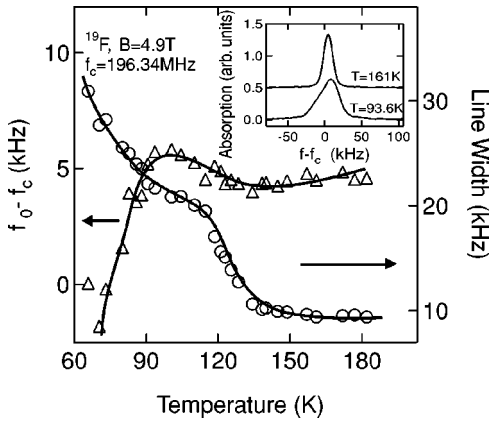

FIG. 3. First moment (f_0) and linewidth, evaluated from the ^{19}F spectra. The first moment is measured relative to f_c; see the text for a definition of the linewidth. The solid lines serve as guides to the eye. Examples of the ^{19}F spectra appear in the inset.

shape. There is no observable change at T_{CO}. However, from approximately $T=130$ K and below, changes in both the first moment and linewidth are noticeable. The definition of the linewidth we have used is the frequency span that includes half of the integrated intensity. Changes appear to occur in two steps, the first in a temperature range centered about $T=120$ K and the second in a temperature range around $T=75-80$ K.

In the discussion that follows, the ^{13}C data is used to construct the phase diagram, and observations from both ^{13}C and ^{19}F NMR motivate linking of the counterion motion to the stabilization of the CO. The ^{13}C 2D NMR spectra we have presented appear quite different from each other. The doubling of the number of shifts is a result of charge disproportionation in which two different molecular environments emerge below a phase transition temperature T_{CO}.[2] At ambient pressure, we find $T_{CO}=156$ K, which coincides with the onset of insulating behavior in transport studies.[16] At high pressure ($P>0.5$ GPa), evidence for charge disproportionation is not resolved. Further, the appearance of the peaks separated along the f_1 axis by $(3/2)\Delta f_d$ is precisely that seen for the spin-Peierls compound $(TMTTF)_2AsF_6$.[2] In other words, at high pressures, the ground state of $(TMTTF)_2SbF_6$ is no longer CO or AF, but has properties similar to the spin-Peierls (SP) compound.

Collecting data over a range of pressures leads us to the phase diagram shown in Fig. 4. As the pressure is increased, the ordering temperature T_{CO} to the CO state decreases. T_{CO} is reduced by almost half, to 90 K, with 0.5 GPa applied pressure. Over the same pressure range, the charge order amplitude at low temperatures is significantly reduced, and becomes unidentifiable at pressures beyond it. As a consequence, the actual transition line is not established beyond 0.5 GPa. Also decreasing is the AF ordering temperature T_N. When $P>0.4$ GPa, no experimental signature for the AF state is observed. For technical reasons associated with the experiments that are perhaps complicated by quenched disorder, we have not identified a phase boundary for the ground state found at high pressures. Rather, the results of experiments conducted in the range of $T=2-5$ K exhibit the signatures of a singlet ground state.[17]

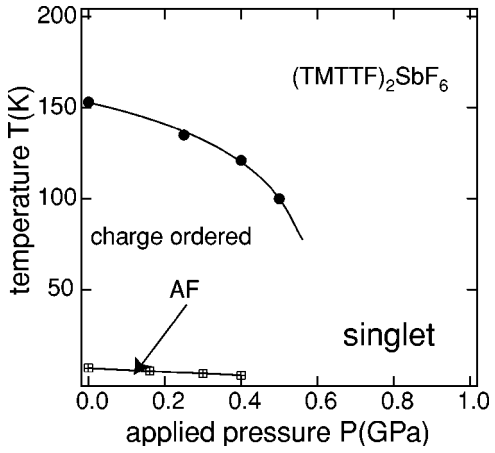

FIG. 4. Pressure vs temperature phase diagram for $(TMTTF)_2SbF_6$ identified using ^{13}C NMR spectroscopy.

Now we would like to discuss the significance of the ^{19}F data in the context of the phase diagram. We first consider the nature of the ^{19}F linewidth broadening. It is natural, at least in part, to consider the spectral effects as related to motion of the SbF_6^- counterion. More generally, the counterions of the TMTTF and TMTSF salts fall into two classes: centrosymmetric and noncentrosymmetric. In the first class are the hexaflourides PF_6^-, AsF_6^-, and SbF_6^-, and Br^-, and in the second are ClO_4, FSO_3, etc. All are small and compact; SbF_6^- is one of the largest, with the F-Sb-F linear distance approximately 3.8 Å. At high temperatures the orientation of the counterions is known to be highly disordered, and thought to be rotating.[18] Upon cooling, the noncentrosymmetric counterions orientationally order[19] at a first-order phase transition. At this transition the space group symmetry of the crystal is lowered. The centrosymmetric ions are not reported to do that; instead, their motions are considered activated so line broadening is expected to occur as a crossover upon cooling and there is no broken symmetry. At first glance, our results appear inconsistent with this scenario because the line shape is asymmetric. In a single crystal, this would indicate highly disordered sites at low temperatures, and the resulting variation of chemical or Knight shifts. From the data, we see that a distribution of chemical shifts is not observable (the line is homogeneously broadened). The broadening results when anionic motions become suitably slow or a first-order ordering transition of some kind takes place. The additional broadening that occurs at lower temperatures in the ^{19}F linewidth appears to be associated with dynamics of some of the methyl groups and ^1H-^{19}F coupling. As evidence, we note that there is a strong peak in the ^1H spin lattice relaxation in the same temperature range, and is very similar in strength and temperature range to what is observed in the TMTSF salts.[18]

It is natural to associate the decrease in the CO order parameter, from Fig. 1, with the ^{19}F line broadening and shift. For the broadening to occur, the anions must be stationary on a time scale of the order of the inverse (high temperature) homogeneous linewidth,[20] which can occur through an activated diffusion process or as a result of a structural phase transition. For either case, the behavior of the order parameter suggests that suppression of the counterion motion, or the disorder associated with it, leads to suppression of the charge disproportionation on the donor molecules.

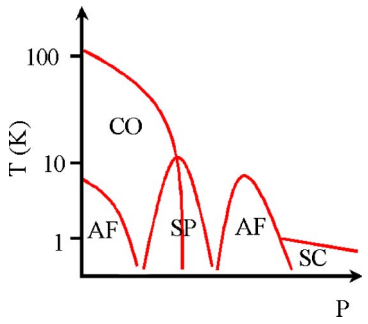

FIG. 5. (Color online) A proposed generic phase diagram for the TMTTF and TMTSF salts.

Finally, we address the evolution with pressure of both the CO order parameter and the ground states. In Fig. 4, neither the line marking the transition to the CO phase nor the CO/AF line is followed to $T=0$. In transport experiments,[21] there is an indication that the dielectric and resistive anomalies associated with the transition to the CO phase are monotonically suppressed with applied pressure. Our own transport studies confirm this. In the ^{13}C NMR spectrum, we observe some broadening of the spectral features, along with a weakening of the CO order parameter as pressure is increased. Beyond $P \approx 0.5$ GPa, the CO features are unresolved. At the same time, the temperature at which ^{121}Sb line broadening is observed coincides with the ^{19}F broadening and *increases* with pressure.[22] These observations suggest that there is a phase competing with the CO, and its stability is associated with counterion degrees of freedom.

To see how the counterion can play a role, we consider first the simplest model producing the CO: the quasi-one-dimensional extended Hubbard model, including only electronic degrees of freedom.[4] With large enough on-site and near-neighbor repulsions U and V (relative to hopping integral t) in 1/4-filled systems, a charge pattern of alternating rich and poor sites is produced and the ground state is antiferromagnetic. Nevertheless, there are no diffraction experiments identifying the order parameter, and including electron-lattice coupling leads to other possibilities for the charge configuration of the CO state.[9] It is also argued that the physically appropriate values for V may not exceed the threshold for the charge order of the extended Hubbard model.[6,7,9] Producing ferroelectricity, as inferred from low-frequency dielectric experiments,[3] from the CO phase requires more couplings. Including a coupling term between the electrons in the stack and the charged counterion naturally gives rise to ferroelectric order parameters.[6,8] Peierls-type coupling to the lattice leads to order parameters reminiscent of the spin-Peierls order.[5,23] Then, it follows that a large-amplitude CO results from coupling to the counterion. It competes with the instrastack Peierls coupling, which produces the SP ground state.[24] Experimental evidence for the competition between the CO- and SP-order parameters was seen previously in experiments on $(TMTTF)_2AsF_6$.[12] To ex-

plain the obervations reported here, we propose that the relative importance of the anion coupling is diminished once the anions freeze into place. That is, the freezing of the rotations limits in some way the motion of the counterion. In turn, the coupling is reduced and the CO phase is destabilized. Applied pressure, as revealed by ^{121}Sb NMR, suppresses the anion rotation,[22] and consequently destabilizes the CO and AF phases.

To conclude, we offer a generic phase diagram for the TMTTF and TMTSF salts that incorporates our observations for the SbF_6 salt. At low chemical pressure, the donor stacks are strongly dimerized, $T_{CO}=156$ K, and the ground state is antiferromagnetic. Increasing pressure leads to a frustration of the CO resulting from a modified coupling to the counterion, and once it is sufficiently suppressed the ground state is singlet (spin-Peierls) rather than antiferromagnetic. The observation that for $(TMTTF)_2SbF_6$ $dT_N/dP<0$ is presumably associated with a competition with this nonmagnetic ground state found at higher pressure. Further pressurization leads to the familiar sequence: another AF state and superconductivity. It is reasonable to ask whether this second, higher-pressure AF state is a reentrance of the phase described in Fig. 4, or whether it is a distinctly different symmetry breaking. The salts $(TMTTF)_2Br$ and $(TMTSF)_2PF_6$ should provide the answer, as they are understood to be representative of that portion of the phase diagram where the second AF phase appears. X-ray scattering results[25] from the two materials provide evidence for a coexistence of weak charge and bond modulations, suggesting an even richer evolution of the phases than is presented in Fig. 5.

The research was supported by the National Science Foundation under Grant No. DMR-0203806. The authors are grateful for conversations with S. Brazovskii, S. Mazumda, P. Monceau, and H. Seo.

*Electronic address: weiqiang@physics.ucla.edu

[1] D. Jerome and H. J. Schultz, Adv. Phys. **51**, 293 (2002).
[2] D. S. Chow, F. Zamborszky, B. Alavi, D. J. Tantillo, A. Baur, C. A. Merlic, and S. E. Brown, Phys. Rev. Lett. **85**, 1698 (2000).
[3] P. Monceau, F. Y. Nad, and S. Brazovskii, Phys. Rev. Lett. **86**, 4080 (2001).
[4] H. Seo and H. Fukuyama, J. Phys. Soc. Jpn. **66**, 1249 (1997).
[5] S. Mazumdar, S. Ramasesha, R. T. Clay, and D. K. Campbell, Phys. Rev. Lett. **82**, 1522 (1999).
[6] J. Riera and D. Poilblanc, Phys. Rev. B **63**, 241102 (2001).
[7] R. T. Clay, S. Mazumdar, and D. K. Campbell, Phys. Rev. B **67**, 115121 (2003).
[8] S. Brazovskii, P. Monceau, and F. Nad, Synth. Met. **137**, 1331 (2003).
[9] S. Mazumdar, R. T. Clay, and D. K. Campbell, Phys. Rev. B **62**, 13400 (2000).
[10] F. Y. Nad and P. Monceau, J. Phys. IV **12**, 133 (2002).
[11] T. Nakamura, J. Phys. Soc. Jpn. **72**, 213 (2003).
[12] F. Zamborszky, W. Yu, W. Raas, S. E. Brown, B. Alavi, C. A. Merlic, and A. Baur, Phys. Rev. B **66**, 081103 (2002).
[13] C. A. Merlic, A. Baur, D. J. Tantillo, and S. E. Brown, Synth. Commun. **29**, 2953 (1999).
[14] R. R. Ernst, G. Bodenhausen, and A. Wokaun, *Principles of Nuclear Magnetic Resonance in One and Two Dimensions* (Oxford University Press, Oxford, 1990), pp. 360–366.
[15] The dipole coupling frequency Δf_d is slightly different between Fig. 1 and Fig. 2 because of a 60° rotation of the crystal axis relative to the magnetic field direction.
[16] C. Coulon, S. S. P. Parkin, and R. Laversanne, Phys. Rev. B **31**, 3583 (1985).
[17] W. Yu, F. Zamborszky, B. Alavi, A. Baur, C. A. Merlic, and S. E. Brown, J. Phys. IV **114**, 35 (2004).
[18] V. J. McBrierty, D. C. Douglass, F. Wudl, and E. Aharon-Shalom, Phys. Rev. B **26**, 4805 (1982).
[19] J. P. Pouget and S. Ravy, J. Phys. I **6**, 1501 (1996).
[20] C. P. Slichter, *Principles of Nuclear Magnetic Resonance* 3rd ed. (Springer-Verlag, Berlin, 1996), pp. 592–595.
[21] P. Monceau (private communication).
[22] W. Yu, F. Zhang, F. Zamborszky, B. Alavi, A. Baur, C. A. Merlic, and S. E. Brown (unpublished).
[23] J. Riera and D. Poilblanc, Phys. Rev. B **62**, R16 243 (2000).
[24] M. Kuwabara, H. Seo, and M. Ogata, J. Phys. Soc. Jpn. **72**, 225 (2003).
[25] J. P. Pouget and S. Ravy, Synth. Met. **85**, 1523 (1997).